

Improving the Power of a Two-Sample Graph Test with Applications in Connectomics

Jaewon Chung^{1,†}, Bijan Varjavand^{1,†}, Jesús Arroyo^{1,2}, Anton Alyakin¹, Joshua Agterberg¹, Minh Tang³, Joshua T. Vogelstein^{1,*}, Carey E. Priebe¹

Abstract. In many applications, there is interest in testing whether two graphs come from the same distribution. However, due to the nature of graph data, classical statistical methods are not directly applicable. When the distribution of each graph is determined by a distribution for vertex latent positions, in particular under the random dot product graph model, a statistical procedure is derived to test whether the two sets of latent positions are equally distributed. We empirically analyze several methods for this problem, and show that adapting Optimal Transport Procrustes (OPT) for aligning latent positions and multiscale graph correlation (MGC) for hypothesis testing to answer this question results in a test which outperforms several existing methods.

Keywords: Distance correlation, multiscale graph correlation, brain networks.

1 Introduction Graphs are a useful data type because they naturally encode information about relationships between variables. Statistical network analysis is becoming an increasingly relevant area [1], as well as applications in other fields such as brain science [2] or social sciences [3]. Often, we encounter more than one graph observation, and it is statistically and scientifically interesting to determine whether the two graphs come from the same distribution: the *graph hypothesis testing* problem. When the two samples are real-valued scalars, procedures such as the *t*-test and Wilcoxon rank-sum test are available, but these methods do not generalize to more complex data types such as graphs.

Recently, methods have been proposed for determining whether two graphs are statistically equivalent under different settings [4–14]. Most of these methodologies are aimed for pairs of graphs with a known correspondence between their vertices, and thus the problem consist in finding significant differences on the corresponding edges or vertices. Here, we focus on the more general setting where this vertex correspondence is unknown or might not exist, for example when the graphs do not have the same number of vertices. In this setting, we are interested in identifying significant differences on some underlying structure on the vertices. In particular, [6] proposed a nonparametric approach able to operate on graphs with unmatched vertex sets based on the concept of distance between probability distributions on a vertex latent space. This method uses the maximum mean discrepancy (MMD) test to detect differences between distributions of the latent positions of the vertices. MMD has been shown to be equivalent to the Energy distance two-sample test, the Hilbert-Schmidt independence criterion (HSic), and the distance correlation test for independence (DCorr) [15, 16]. Here, HSic and DCorr, which are independence tests, are used as two-sample tests via first performing a *k*-sample transform, which consists of concatenating the two samples, defining an auxiliary label vector, and subsequently testing for independence of those [16].

Multiscale graph correlation (MGC) is a recently proposed measure of dependence that has shown an improved empirical power by intelligently selecting the appropriate scale of the data [17–19]. In this paper, we empirically show that MGC also outperforms DCorr in two-sample graph hypothesis testing.

2 Background

*Corresponding author: jovo@jhu.edu; †These authors contributed equally

¹ Johns Hopkins University, Baltimore, MD 21218, United States

² University of Maryland, College Park, MD 20742, United States

³ North Carolina State University, Raleigh, NC 27695, United States

2.1 Graphs and Embeddings A graph $G = (\mathbb{V}, \mathbb{E})$ with n vertices is composed of a vertex set $\mathbb{V} = \{v_1, \dots, v_n\}$ and an edge set $\mathbb{E} \subseteq \mathbb{V} \times \mathbb{V}$, where the edge $(v_i, v_j) \in \mathbb{E}$ connects vertices i and j . Graphs can be represented by an adjacency matrix $A \in \{0, 1\}^{n \times n}$, with rows and columns corresponding to vertices and matrix entries corresponding to edge values, so $A_{ij} = 1$ whenever $(v_i, v_j) \in \mathbb{E}$.

The *random dot product graph* (RDPG) model [20] treats the entries of an adjacency matrix A as independent Bernoulli random variables, where the probability of an edge is given by the dot product of pairs of latent positions $x_1, \dots, x_n \in \mathbb{R}^d$ for each vertex, so $\mathbb{P}(A_{ij} = 1) = x_i^T x_j$. These latent positions are independent random variables sampled according to some distribution F . Writing $X = [x_1 \cdots x_n]^T$ as the matrix of latent positions, we denote by $(X, A) \sim \text{RDPG}(n, F)$ a RDPG with adjacency matrix A and (usually unobserved) latent positions X sampled from F .

The RDPG model provides a flexible framework for studying the statistical equivalence of a pair of graphs. Suppose that $(X, A) \sim \text{RDPG}(n, F_X)$ and $(Y, B) \sim \text{RDPG}(m, F_Y)$. Then, the two graphs A and B are said to have the same distribution if $F_X = F_Y$, up to an orthogonal transformation due to the nonidentifiability inherent with inner products [6]. Formally, this hypotheses test can be stated as

$$\begin{aligned} H_0 : F_X &= F_Y \circ W && \text{for some orthogonal operator } W \\ H_A : F_X &\neq F_Y \circ W && \text{for all orthogonal operators } W. \end{aligned}$$

The graphs A and B do not need to have matched vertices, or the same number of vertices, because we are comparing distributions of latent positions, not the latent positions themselves.

Latent positions are typically unobserved in practice and can be estimated via the *adjacency spectral embedding* (ASE) [21]. Suppose that $A = USV^T + U_\perp S_\perp V_\perp^T$ is the singular value decomposition of A , where $U, V \in \mathbb{R}^{n \times d}$, $U_\perp, V_\perp \in \mathbb{R}^{n \times (n-d)}$ are jointly orthogonal matrices corresponding to the singular vectors of A , and $S \in \mathbb{R}^{d \times d}$, $S_\perp \in \mathbb{R}^{(n-d) \times (n-d)}$ are diagonal matrices such that S contains the d largest singular values of A . Then, the ASE of A is defined as $\hat{X} = US^{1/2}$. This simple and computationally efficient approach results in consistent estimates \hat{X} and \hat{Y} of the true latent positions X and Y [21–23]. If the two networks have different number of vertices, it is recommended to first correct for the difference in variance of the two estimates, as otherwise the subsequent testing procedure might be invalid. For more on this correction see [24].

The ASE depends on the embedding dimension d ; in practice, we select this dimension via the scree plot of the eigenvalues of the adjacency matrix which can be done automatically via a likelihood profile approach [25].

2.2 Orthogonal Nonidentifiabilities There are two sources of an orthogonal nonidentifiability associated with using the ASE in RDPG [26]. The first is associated with the RDPG model itself, and can take a form of any orthogonal transformation, since for any orthogonal matrix W , it holds that $(XW)(XW)^T = XWW^T X^T = XX^T$. When using ASE, this orthogonal matrix converges to a population value at the rate $O_p(n^{-1/2})$, and, thus, rarely has any inferential consequences [6, 26].

The second source, called subspace nonidentifiability, is associated with taking a singular value decomposition as a part of ASE. Recall that if the singular values are not repeated, then the associated singular vector is determined only up to a sign ambiguity. This sign ambiguity is often adjusted for by flipping the signs of each dimension such that the medians have the same sign; that is for each embedding dimension, $\text{sgn}(\text{med}(X_i)) = \text{sgn}(\text{med}(Y_i))$ for all $i \in d$ [6, 24]. This heuristic can perform poorly when the medians of the samples are too close to zero. Furthermore, for a case of repeated eigenvalues, this approach falls short, since the singular values associated with such values are non-

identifiable up to a more general rotation. That is, this subspace nonidentifiability has a block-diagonal, rather than a simple diagonal structure [26].

If the two graphs had paired vertices, then the orthogonal misalignment, even a block-diagonal one, between the two samples could be resolved by using a solution to a well-known orthogonal Procrustes problem [27]. In unpaired graphs, we can employ an Optimal Transport Procrustes (OTP) algorithm [28], which simultaneously solves the alignment and the assignment problems. Formally, this algorithm minimizes the objective function

$$(2.1) \quad \min_{W, \Pi} \langle \Pi, C_W \rangle$$

where the entries of the cost matrix C_W are given by $(C_W)_{ij} = \|\hat{X}_i - W\hat{Y}_j\|^2$, $\hat{X} \in \mathbb{R}^{n \times d}$ and $\hat{Y} \in \mathbb{R}^{m \times d}$ are estimated latent positions, $\Pi = \frac{1}{nm} \vec{1} \vec{1}^T$ is an assignment matrix that satisfies $\Pi \vec{1} = \frac{1}{n} \vec{1}$ and $\Pi^T \vec{1} = \frac{1}{m} \vec{1}$, and W is constrained to be orthogonal. Given an initial guess W_0 , the algorithm iteratively updates $\Pi_{i+1} | W_i$ by via an optimal transport algorithm [29] and $W_{i+1} | \Pi_i$ using the solution to the Procrustes problem. In graph setting, the algorithm is initialized with all possible orthogonal diagonal matrices, i.e. the 2^d different diagonal matrices with ± 1 on the diagonal [28].

2.3 Distance Correlation Due to the equivalence between two-sample and independence testing [16], distance correlations (DCorr) can be used to test the equality of the distributions F_X and F_Y . Define $Z = (X^T, Y^T)^T \in \mathbb{R}^{N \times d}$ and $E = (0_n, 1_m)^T \in \mathbb{R}^N$, where $N = n + m$. DCorr tests the independence of Z and E using some distance functions $\delta_Z : \mathbb{R}^d \times \mathbb{R}^d \rightarrow \mathbb{R}$ and $\delta_E : \mathbb{R} \times \mathbb{R} \rightarrow \mathbb{R}$. First, DCorr computes distance matrices D^Z, D^E such that $D_{i,j}^Z = \delta_Z(Z_i, Z_j)$ and $D_{i,j}^E = \delta_E(E_i, E_j)$. The distance matrices are then doubly centered to $D^{Z'}, D^{E'}$, where $D_{i,j}^{Z'} = D_{i,j}^Z - \overline{D^Z}_{\cdot,j} - \overline{D^Z}_{i,\cdot} + \overline{D^Z}_{\cdot,\cdot}$, and similarly for $D^{E'}$. Here the column means, row means, and the grand mean are $\overline{D^Z}_{\cdot,j} = \frac{1}{N} \sum_{i=1}^N D_{i,j}^Z$, $\overline{D^Z}_{i,\cdot} = \frac{1}{N} \sum_{j=1}^N D_{i,j}^Z$, and $\overline{D^Z}_{\cdot,\cdot} = \frac{1}{N^2} \sum_{i=1}^N \sum_{j=1}^N D_{i,j}^Z$, respectively. The sample DCorr test statistic [30] is defined as

$$\text{DCorr}(Z, E) = \frac{1}{N(N-3)\sigma_{D^{Z'}}\sigma_{D^{E'}}} \sum_{i,j} D_{i,j}^{Z'} D_{i,j}^{E'}$$

where $\sigma_{D^{Z'}}$ and $\sigma_{D^{E'}}$ are the standard deviation of values in $D^{Z'}$ and $D^{E'}$, respectively. A null distribution of this test statistic can be generated by permuting the indices of E or approximated using an asymptotic result.

The centered versions $D^{Z'}, D^{E'}$ have the property that all rows and columns sum to zero, but the test statistic is biased for finite samples. An unbiased version of DCorr modifies the centering method of the pairwise distance matrices [30]. This method, called U-centering, generates a matrix $D^{Z''}$ that has the additional property that $E[D_{i,j}^{Z''}] = 0, i, j = 1, \dots, N$. $D^{Z''}$ uses a slightly different form for the row means, column means, and grand mean, given by $\widetilde{D^Z}_{\cdot,j} = \frac{1}{N-2} \sum_{i=1}^N D_{i,j}^Z$ (similarly for row means) and $\widetilde{D^Z}_{i,\cdot} = \frac{1}{(N-2)(N-1)} \sum_{i,j} D_{i,j}^Z$. The test statistic is defined analogously modulo these new definitions.

2.4 Multiscale Graph Correlation An alternative method for approaching the hypothesis testing problem is MGC [17–19], which uses the distance based methods in DCorr, but also considers the local scale of the data. MGC is based on unbiased DCorr, resulting in it also being unbiased. MGC consists of the following steps.

1. Compute the centered distance matrices $D^{Z''}$ and $D^{E''}$.
2. For each k, l in $1, \dots, N$, compute the k and l nearest neighbors of each row of $D^{Z''}$ and $D^{E''}$, respectively, and denote the induced nearest neighbor graphs by $G^k \in \{0, 1\}^{N \times N}$ and $H^l \in \{0, 1\}^{N \times N}$.
3. Estimate the local normalized correlations $c^{k,l}$ such that

$$c^{kl} = \frac{\sum_{i,j} D_{ij}^{Z''} D_{ij}^{E''} G_{ij}^k H_{ij}^l}{\left(\sum_{i,j} (D_{ij}^{Z''})^2 G_{ij}^k \right) \left(\sum_{i,j} (D_{ij}^{E''})^2 H_{ij}^l \right)}.$$

4. Using a smoothing parameter τ , estimate the smoothed maximum of c^{kl} over all possible values of k and l , defined as

$$R = \text{LCC}\{(k, l) : c^{kl} > \max(\tau, c^{NN})\},$$

$$c^* = \max_{(k,l) \in R} c^{kl},$$

where LCC denotes the largest connected component of the graph defined by a set of edges. Once the MGC test statistic c^* is obtained, a permutation test is performed to determine the null distribution. When the relationship is nonlinear or non-monotonic, MGC tends to choose scales smaller than n , detecting relationships more often than DCorr. It can be considered a direct upgrade to the above methods at a minor running time cost [17].

3 Simulations The performance of DCorr and MGC is analyzed by simulating different graphs. The graphs are simulated according to the RDPG model, using different distributions (described below) to generate their latent positions $X = (x_1, \dots, x_n)^T$ and $Y = (y_1, \dots, y_n)^T$, and the latent positions are estimated via ASE with embedding dimension $\hat{d} = 1$. The sign ambiguity is resolved via median flip since the graphs are embedded into one dimension. The estimates are then used to compute the corresponding test statistics, and calculate the p -value after estimating the null distribution via permutation test. The tests reject at a significance level $\alpha = 0.05$, and the empirical power is based on 1000 Monte Carlo replicates. This process is repeated for increasing numbers of vertices in each graph. The graph generating mechanisms are described next.

3.1 Equal distribution of the latent positions First, we analyze the performance of the methods when the null hypothesis is true, so the latent positions X and Y have the same distribution: $x_i \stackrel{\text{iid}}{\sim} F_X$ and $y_i \stackrel{\text{iid}}{\sim} F_X$, $i = 1, \dots, n$, with $F_X = \text{Unif}(.2, .7)$. That is, these mutually independent sets of latent positions are uniformly distributed on the range $(.2, .7)$. Figure 1 (left) shows the empirical power of the tests for different numbers of vertices. The empirical power does not exceed α , showing that both DCorr and MGC correctly control the type I error.

3.2 Linear difference in the distributions For this setting, we generate $x_i \stackrel{\text{iid}}{\sim} F_X$ and $y_i \stackrel{\text{iid}}{\sim} F_X + 0.1$. The results of this setting are shown in Figure 1 (middle). As the number of vertices in each graph increases, the difference between the distributions becomes easier to detect, and both DCorr and MGC algorithms detect the differences, resulting in power increasing to unity.

3.3 Nonlinear difference in the distributions Finally, set $x_i \stackrel{\text{iid}}{\sim} F_X$ and $y_i \stackrel{\text{iid}}{\sim} 0.5 \text{Beta}(.2, .2) + 0.2$. Figure 1 (right) shows similar behavior to the previous linear scenario, in which the power of both DCorr and MGC goes to 1, but MGC dominates DCorr at smaller sample sizes.

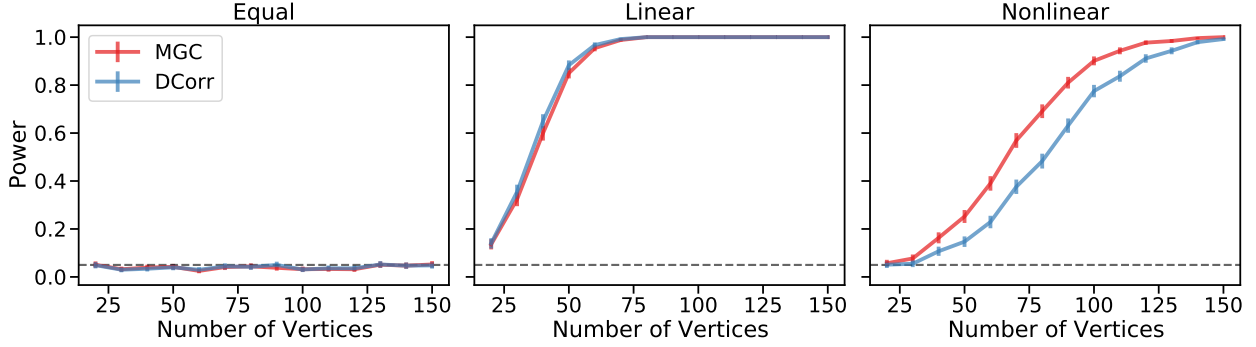


Figure 1: Empirical power of different methods (DCorr and MGC) for detecting differences in the distribution of latent positions as a function of the number of vertices. Dashed lines represent $\alpha = 0.05$ and error bars represent 95% confidence interval. (Left) When the distributions of the latent positions are identical, both methods are valid as power is near or at $\alpha = 0.05$. (Middle) When the distributions are linearly dependent, both methods are equally powerful and consistent. (Right) When the distributions are nonlinearly dependent, both methods are consistent, but MGC is more powerful than DCorr.

4 Synthetic and Real Data Applications In this section, we discuss applications to synthetic and real data using the *Drosophila melanogaster* connectomes.

4.1 Drosophila melanogaster Brain The connectomes, or graphs, of the *Drosophila melanogaster* mushroom body have been obtained in [31]. The left brain graph (A^L) has $n = 163$ neurons/vertices and the right brain graph (A^R) has $m = 158$ neurons/vertices. Both graphs are binary with $A_{ij} \in \{0, 1\}$, symmetric with $A = A^\top$, and hollow with $\text{diag}(A) = \vec{0}$. The edges of the data represent whether a synaptic connection exist between a pair of neurons or not.

4.2 Synthetic Data Analysis The performance of the two SVD alignment methods (median flipping and Optimal Transport Procrustes) and two hypothesis tests (DCorr and MGC) is analyzed by simulating synthetic data from the *Drosophila* connectomes. That is, given an estimated latent positions $\hat{X} \in \mathbb{R}^{n \times d}$, two sets of latent positions are sampled, one with and one without perturbation to analyze the power of various methods as a function of both effect size, or the magnitude of perturbation, and the number of vertices that are perturbed.

The first step in data generation is to estimate the point-wise covariance matrix, $\hat{\Sigma}(\hat{X}_i)$ of each row of \hat{X}_i , given by the central limit theorem [20]. New latent positions are sampled from $\mathcal{MVN}(\hat{X}_i, \hat{\Sigma}(\hat{X}_i))$ where $i \in \mathcal{P}$ and \mathcal{T} is the set of vertices chosen for sampling new latent positions, and \mathcal{MVN} is the multivariate normal distribution. We consider two options for sampling \mathcal{P} : sampling without replacement, wherein the indices of which row of latent position and covariance is sampled without replacement (SRSWOR), and sampling with replacement, wherein the indices are sampled with replacement (SRSWR).

In sampling without replacement, the vertex set is defined as $\mathcal{P} = [n]$. Two new latent positions are sampled via $V \sim \mathcal{MVN}(\hat{X}_i, \hat{\Sigma}(\hat{X}_i))$ and $W \sim \mathcal{MVN}(\hat{X}_i + \epsilon_j, \hat{\Sigma}(\hat{X}_i))$ for $i \in \mathcal{P}$ and ϵ_j denotes the perturbation applied to random subset $\mathcal{O} \subseteq \mathcal{P}$. The perturbation is defined as

$$\epsilon_j \sim \begin{cases} \mathcal{S}_r^d, & \text{if } j \in \mathcal{O} \\ \vec{0}, & \text{otherwise} \end{cases}$$

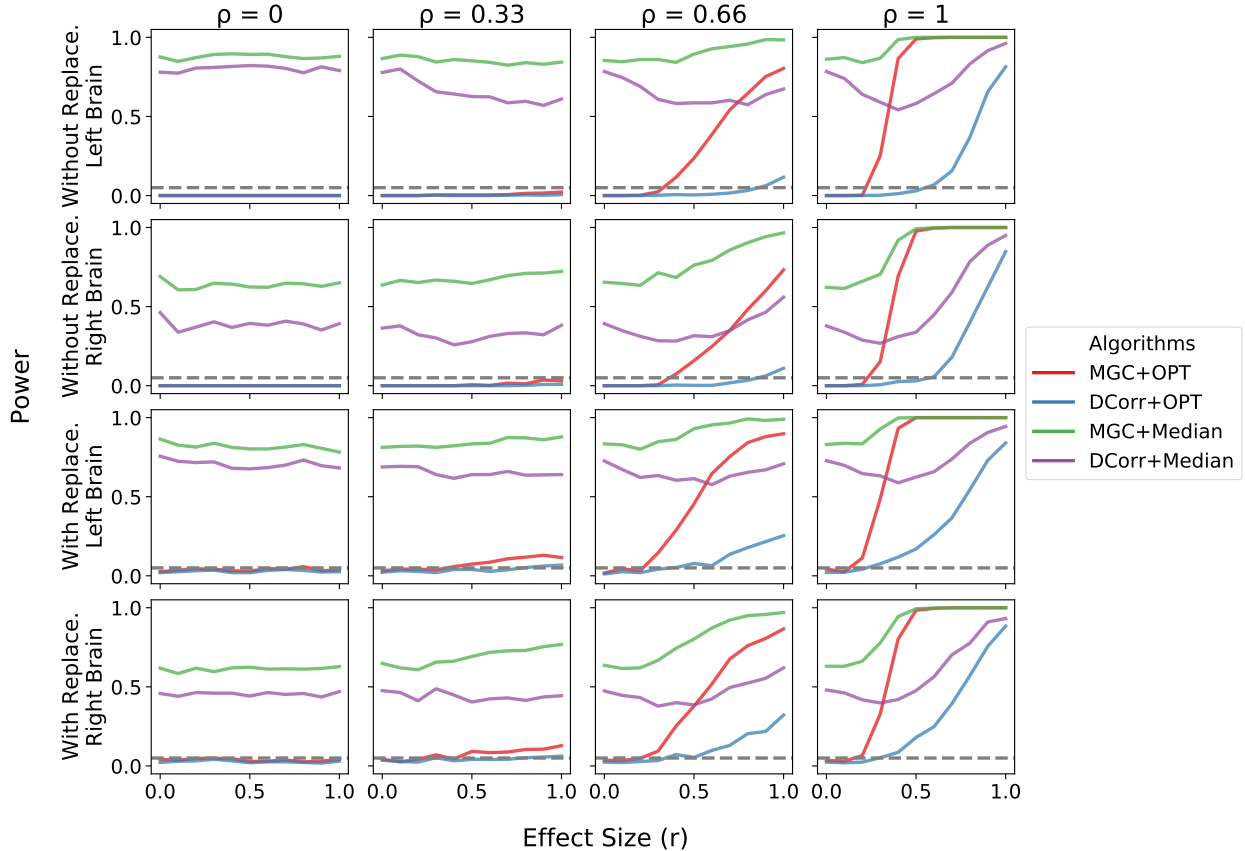


Figure 2: Power vs. effect size using synthetic data generated from *Drosophila* connectomes. Each row represents right or left hemisphere of the brain and a sampling method. Each line represents an algorithm, and x-axis is the magnitude, or the effect size (r), of the change in latent positions. Each column represents different proportion of vertices changed. Thus, when $\rho = 0$, the distributions F_V and F_W are the same. The gray dashed line is $\alpha = 0.05$. Testing via median flip is invalid as shown in first column ($\rho = 0$), but OPT resolves the inadequacy of median flip. Testing via MGC is more powerful than testing via DCorr as shown in columns where $\rho > 0$.

where \mathcal{S}_r^d is a d dimensional sphere with radius r . Thus, r represents the effect size, and $\rho = |\mathcal{O}|/n$ is the proportion of changed vertices. In sampling with replacement, the vertex set is defined as $\mathcal{P} = \text{SRSWR}(n, [n])$, and the latent position sampling proceeds similarly.

Once new latent positions are sampled, two adjacency matrices A and B are sampled via $(V, A) \sim \text{RDPG}(n, F_V)$ and $(W, B) \sim \text{RDPG}(n, F_W)$. The hypothesis $H_0 : F_V = F_W$ vs $F_V \neq F_W$ is tested by estimating the latent positions via ASE then using both alignment methods (median flip and Optimal Transport Procrustes) and test methods (DCorr and MGC). The hypotheses reject at a significance level $\alpha = 0.05$, and the empirical power based on 500 Monte Carlo replicates is reported. This process is repeated for increasing effect size with $r \in [0, 1]$ and increasing proportion of changed vertices with $\rho \in [0, 1]$ for both left and right *Drosophila* mushroom body.

Figure 2 shows that median flip invalidates both DCorr and MGC. When $r = 0$, both V and W are sampled from same distribution, but results in power > 0.05 . OPT resolves the inadequacy of the median flip as power is near $\alpha = 0.05$. In addition, as the effect size increases and the proportion of

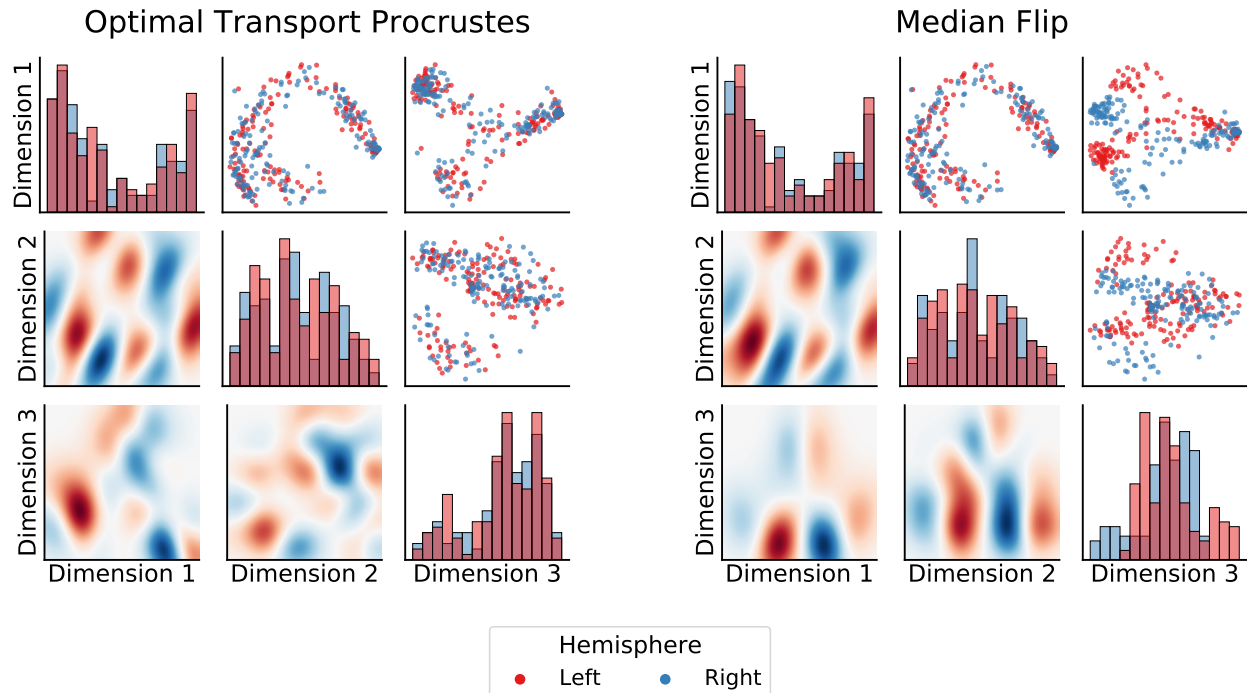


Figure 3: Embeddings for the *Drosophila* connectomes after alignment with Optimal Transport Procrustes and median flip. The diagonals are histograms of each dimension, upper off-diagonals are pairwise scatter plots, and lower off-diagonals are the difference of the kernel density estimates of the two embeddings. (Left) OPT aligns all three dimensions properly. (Right) Median flips results in misalignment in dimension 3 of the left hemisphere embedding.

vertices that are changed increases, power increases to unity. Lastly, MGC dominates DCorr as power increases to unity faster.

4.3 Left vs Right *Drosophila* Brain The left and right *Drosophila* mushroom body are similar, but not identical as some neurons exist in one hemisphere may not exist in the other. To compare between these hemispheres, we test the difference of the distributions of the graph of the left mushroom body (L) and the graph of the right mushroom body.

The ASE embeddings of each hemisphere are denoted by \hat{X}_L and \hat{X}_R , estimating latent positions of RDPG models for each hemisphere, with assumed distributions F_L and F_R respectively. We test the hypothesis $H_0 : F_L = F_R$ vs $H_1 : F_L \neq F_R$. Figure 3 shows pair-plots of the embeddings after alignment with OPT and median flip. Using the estimated latent positions, we test the equality of the distributions using the same methods as before. The null distributions and p -values are shown in Figure 4. As observed in Figure 3, the latent positions of both hemispheres are similar, suggesting there is no difference in the distributions. However, median flip fails due to misalignment in one of the embedding dimensions, resulting in p -values less than 0.01, while testing via OPT results in p -values of 1.

5 Discussion The results presented herein demonstrate the improvement of the original two-sample graph testing by aligning estimated latent positions via Optimal Transport Procrustes and testing via multiscale graph correlation. For applications in connectomics, we show that the orthogonal noniden-

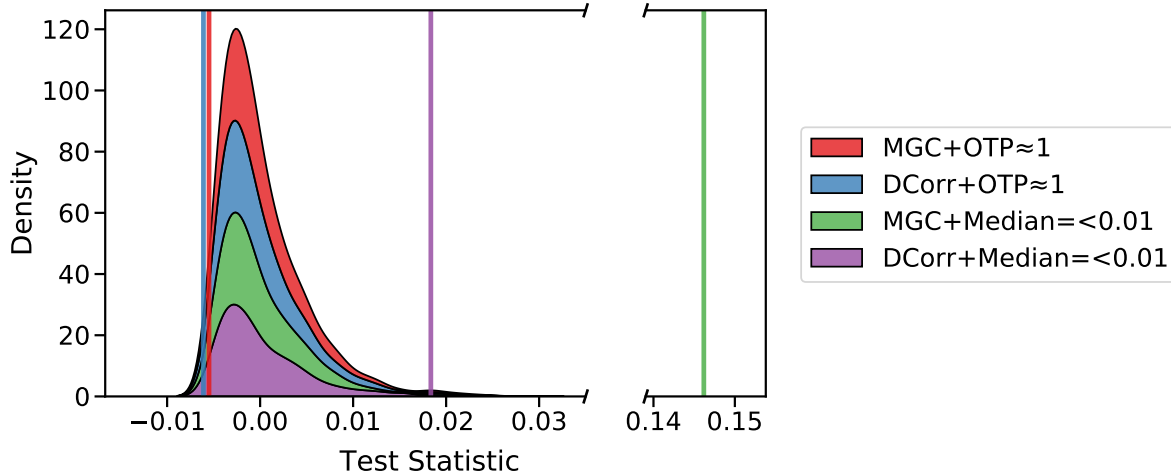


Figure 4: Stacked kernel density estimates of the null distributions and corresponding test statistics (vertical lines) from testing the null hypothesis $F_R = F_L$. The p -values of the tests are shown in the legend. Testing via median flip (denoted *Median*) results in p -values < 0.01 for both DCorr and MGC. On the other hand, testing via Optimal Transport Procrustes (denoted *OTP*) results in p -values of 1.

tifiabilities that arise from adjacency spectral embedding can significantly impacts the results. The synthetic data experiments show that median flip can invalidate DCorr and MGC, but OPT resolves the inadequacy of median flip. Both simulated and synthetic experiments show that MGC is more powerful than DCorr when testing via OPT. Thus, testing via OPT and MGC is not only most powerful, but also most trustworthy.

6 Code The analysis were performed using the `graspologic` [32] and `hyppo` [33] Python packages.

Acknowledgment The authors would like to thank the NeuroData group for great advice and an equally great working environment. This material is based on research sponsored by the Defense Advanced Research Projects Agency (DARPA) Lifelong Learning Machines program through contract FA8650-18-2-7834, the National Science Foundation award DMS-1921310, by funding from Microsoft Research, and by the Air Force Research Laboratory and DARPA under agreement number FA8750-20-2-1001. The U.S. Government is authorized to reproduce and distribute reprints for Governmental purposes notwithstanding any copyright notation thereon. The views and conclusions contained herein are those of the authors and should not be interpreted as necessarily representing the official policies or endorsements, either expressed or implied, of the Air Force Research Laboratory and DARPA or the U.S. Government

References

- [1] Anna Goldenberg, Alice X. Zheng, Stephen E. Fienberg, and Edoardo M. Airoldi. A survey of statistical network models. *Found. Trends Mach. Learn.*, 2(2):129–233, February 2010. ISSN 1935-8237. doi: 10.1561/2200000005. URL <http://dx.doi.org/10.1561/2200000005>.
- [2] Ed Bullmore and Olaf Sporns. Complex brain networks: graph theoretical analysis of structural and functional systems. *Nature reviews neuroscience*, 10(3):186, 2009.
- [3] Stanley Wasserman, Katherine Faust, et al. *Social network analysis: Methods and applications*, volume 8. Cambridge university press, 1994.
- [4] Minh Tang, Avanti Athreya, Daniel L. Sussman, Vince Lyzinski, Youngser Park, and Carey E. Priebe. A semiparametric two-sample hypothesis testing problem for random graphs. *Journal of Computational and Graphical Statistics*, 26(2):344–354, 2017. doi: 10.1080/10618600.2016.1193505. URL <https://doi.org/10.1080/10618600.2016.1193505>.
- [5] K. Levin, A. Athreya, M. Tang, V. Lyzinski, and C. E. Priebe. A central limit theorem for an omnibus embedding of multiple random dot product graphs. In *2017 IEEE International Conference on Data Mining Workshops (ICDMW)*, pages 964–967, 2017. doi: 10.1109/ICDMW.2017.132.
- [6] Minh Tang, Avanti Athreya, Daniel L. Sussman, Vince Lyzinski, and Carey E. Priebe. A nonparametric two-sample hypothesis testing problem for random graphs. *Bernoulli*, 23(3):1599–1630, 08 2017. doi: 10.3150/15-BEJ789. URL <https://doi.org/10.3150/15-BEJ789>.
- [7] Debarghya Ghoshdastidar, Maurilio Gutzeit, Alexandra Carpentier, and Ulrike von Luxburg. Two-sample tests for large random graphs using network statistics. In Satyen Kale and Ohad Shamir, editors, *Proceedings of the 2017 Conference on Learning Theory*, volume 65 of *Proceedings of Machine Learning Research*, pages 954–977, Amsterdam, Netherlands, 07–10 Jul 2017. PMLR. URL <http://proceedings.mlr.press/v65/ghoshdastidar17a.html>.
- [8] Keith Levin and Elizaveta Levina. Bootstrapping networks with latent space structure, 2019. arXiv:1907.10821.
- [9] Jesús Arroyo, Avanti Athreya, Joshua Cape, Guodong Chen, Carey E. Priebe, and Joshua T. Vogelstein. Inference for multiple heterogeneous networks with a common invariant subspace, 2019.
- [10] Andrey Rukhin and Carey E. Priebe. A comparative power analysis of the maximum degree and size invariants for random graph inference. *Journal of Statistical Planning and Inference*, 141(2): 1041 – 1046, 2011. ISSN 0378-3758. doi: <https://doi.org/10.1016/j.jspi.2010.09.013>. URL <http://www.sciencedirect.com/science/article/pii/S0378375810004246>.
- [11] Dena Marie Asta and Cosma Rohilla Shalizi. Geometric network comparisons. In *Proceedings of the Thirty-First Conference on Uncertainty in Artificial Intelligence, UAI’15*, pages 102–110, Arlington, Virginia, United States, 2015. AUAI Press. ISBN 978-0-9966431-0-8. URL <http://dl.acm.org/citation.cfm?id=3020847.3020859>.
- [12] P.-A. G. Maugis, S. C. Olhede, C. E. Priebe, and P. J. Wolfe. Testing for equivalence of network distribution using subgraph counts. *Journal of Computational and Graphical Statistics*, 0(0):1–11, 2020. doi: 10.1080/10618600.2020.1736085. URL <https://doi.org/10.1080/10618600.2020.1736085>.
- [13] Debarghya Ghoshdastidar, Maurilio Gutzeit, Alexandra Carpentier, and Ulrike von Luxburg. Two-sample hypothesis testing for inhomogeneous random graphs, 2019. arXiv:1707.00833.
- [14] Cedric E Ginestet, Jun Li, Prakash Balachandran, Steven Rosenberg, and Eric D. Kolaczyk. Hypothesis testing for network data in functional neuroimaging. *Annals of Applied Statistics*, 11(2): 725–750, 2017. ISSN 19417330. doi: 10.1214/16-AOAS1015. URL <https://projecteuclid.org/>

- [download/pdfview{ }1/euclid.aoas/1500537721](#).
- [15] Cencheng Shen and Joshua T. Vogelstein. The exact equivalence of distance and kernel methods for hypothesis testing, 2018. arXiv:1806.05514.
 - [16] Cencheng Shen, Carey E. Priebe, and Joshua T. Vogelstein. The exact equivalence of independence testing and two-sample testing, 2019. arXiv:1910.08883.
 - [17] J. T. Vogelstein, Q. Wang, E. Bridgeford, C. E. Priebe, M. Maggioni, and C. Shen. Discovering and deciphering relationships across disparate data modalities. *eLife*, 8:e41690, 2019.
 - [18] C. Shen, C. E. Priebe, and J. T. Vogelstein. From distance correlation to multiscale graph correlation. *Journal of the American Statistical Association*, 2019.
 - [19] Y. Lee, C. Shen, C. E. Priebe, and J. T. Vogelstein. Network dependence testing via diffusion maps and distance-based correlations. *Biometrika*, 2019.
 - [20] Avanti Athreya, Donniell E. Fishkind, Minh Tang, Carey E. Priebe, Youngser Park, Joshua T. Vogelstein, Keith Levin, Vince Lyzinski, Yichen Qin, and Daniel L Sussman. Statistical inference on random dot product graphs: a survey. *Journal of Machine Learning Research*, 18(226):1–92, 2018. URL <http://jmlr.org/papers/v18/17-448.html>.
 - [21] Daniel L. Sussman, Minh Tang, Donniell E. Fishkind, and Carey E. Priebe. A consistent adjacency spectral embedding for stochastic blockmodel graphs. *Journal of the American Statistical Association*, 107(499):1119–1128, 2012. doi: 10.1080/01621459.2012.699795. URL <https://doi.org/10.1080/01621459.2012.699795>.
 - [22] Daniel Sussman, Minh Tang, and Carey Priebe. Consistent latent position estimation and vertex classification for random dot product graphs. *IEEE Transactions on Pattern Analysis and Machine Intelligence*, 36:48–57, 2014. doi: 10.1109/TPAMI.2013.135.
 - [23] Vince Lyzinski, Daniel L. Sussman, Minh Tang, Avanti Athreya, and Carey E. Priebe. Perfect clustering for stochastic blockmodel graphs via adjacency spectral embedding. *Electronic Journal of Statistics*, 8(2):2905–2922, 2014. doi: 10.1214/14-EJS978. URL <https://doi.org/10.1214/14-EJS978>.
 - [24] Anton A. Alyakin, Joshua Agterberg, Hayden S. Helm, and Carey E. Priebe. Correcting a nonparametric two-sample graph hypothesis test for graphs with different numbers of vertices, 2020.
 - [25] Mu Zhu and Ali Ghodsi. Automatic dimensionality selection from the scree plot via the use of profile likelihood. *Computational Statistics & Data Analysis*, 51(2):918–930, 2006.
 - [26] Joshua Agterberg, Minh Tang, and Carey E. Priebe. On two distinct sources of nonidentifiability in latent position random graph models, 2020. arXiv:2003.14250.
 - [27] Peter H Schönemann. A generalized solution of the orthogonal procrustes problem. *Psychometrika*, 31(1):1–10, 1966.
 - [28] Joshua Agterberg, Minh Tang, and Carey Priebe. Nonparametric two-sample hypothesis testing for random graphs with negative and repeated eigenvalues. *arXiv preprint arXiv:2012.09828*, 2020.
 - [29] David Alvarez-Melis, Stefanie Jegelka, and Tommi S Jaakkola. Towards optimal transport with global invariances. pages 1870–1879, 2019.
 - [30] G. Székely and M. Rizzo. Partial distance correlation with methods for dissimilarities. *Annals of Statistics*, 42(6):2382–2412, 2014.
 - [31] Katharina Eichler, Feng Li, Ashok Litwin-Kumar, Youngser Park, Ingrid Andrade, Casey M Schneider-Mizell, Timo Saumweber, Annina Huser, Claire Eschbach, Bertram Gerber, et al. The complete connectome of a learning and memory centre in an insect brain. *Nature*, 548(7666):175, 2017.
 - [32] Jaewon Chung, Benjamin D. Pedigo, Eric W. Bridgeford, Bijan K. Varjavand, Hayden S. Helm, and

- Joshua T. Vogelstein. Grasp: Graph statistics in python. *Journal of Machine Learning Research*, 20(158):1–7, 2019. URL <http://jmlr.org/papers/v20/19-490.html>.
- [33] Sambit Panda, Satish Palaniappan, Junhao Xiong, Eric W. Bridgeford, Ronak Mehta, Cencheng Shen, and Joshua T. Vogelstein. hypo: A comprehensive multivariate hypothesis testing python package. 2020.